

See discussions, stats, and author profiles for this publication at: <https://www.researchgate.net/publication/273957023>

# Ionophore-Containing Siloprene Membranes: Direct Comparison between Conventional Ion-Selective Electrodes and Silicon Nanowire-Based Field-Effect Transistors

ARTICLE in ANALYTICAL CHEMISTRY · DECEMBER 2014

Impact Factor: 5.64 · DOI: 10.1021/ac504500s · Source: PubMed

CITATION

1

READS

14

6 AUTHORS, INCLUDING:



Anping Cao

Delft University of Technology

6 PUBLICATIONS 128 CITATIONS

SEE PROFILE



Marleen Mescher

Materials innovation institute M2i

6 PUBLICATIONS 20 CITATIONS

SEE PROFILE



Duco Bosma

Delft University of Technology

5 PUBLICATIONS 6 CITATIONS

SEE PROFILE



J.H. Klootwijk

Philips

73 PUBLICATIONS 696 CITATIONS

SEE PROFILE

# Ionophore-Containing Siloprene Membranes: Direct Comparison between Conventional Ion-Selective Electrodes and Silicon Nanowire-Based Field-Effect Transistors

Anping Cao,<sup>†</sup> Marleen Mescher,<sup>†,‡,§</sup> Duco Bosma,<sup>†</sup> Johan H. Klootwijk,<sup>‡</sup> Ernst J. R. Sudhölter,<sup>†</sup> and Louis C.P.M. de Smet<sup>\*,†</sup>

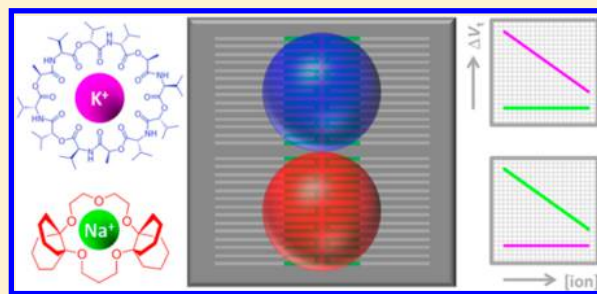
<sup>†</sup>Department of Chemical Engineering, Delft University of Technology, Julianalaan 136, 2628 BL Delft, The Netherlands

<sup>‡</sup>Philips Research Laboratories, High Tech Campus 4, 5656 AE Eindhoven, The Netherlands

<sup>§</sup>Materials innovation institute M2i, Mekelweg 2, 2628 CD Delft, The Netherlands

## Supporting Information

**ABSTRACT:** Siloprene-based, ion-selective membranes (ISMs) were drop-casted onto a field-effect transistor device that consisted of a single-chip array of top-down prepared silicon nanowires (SiNWs). Within one array, two sets of SiNWs were covered with ISMs, each containing two different ionophores, allowing the simultaneous sensing of K and Na ions using a flow cell. It is shown that both ions can be effectively detected in the same solution over a wide concentration range from  $10^{-4}$  to  $10^{-1}$  M without interference. The ISMs were also analyzed in a conventional ISE configuration, allowing a direct comparison. While the responses for  $K^+$  were similar for both sensor configurations, remarkably, the  $Na^+$  response of the ISM-covered SiNW device was found to be higher than the one of the ISE configuration. The addition of a  $Na^+$  buffering hydrogel layer between the  $SiO_2$  of the SiNW and the ISM reduced the response, showing the importance of keeping the boundary potential at the  $SiO_2$ /ISM interface constant. The responses of the siloprene-covered SiNW devices were found to be stable over a period of at least 6 weeks, showing their potential as a multichannel sensor device.



The selective and sensitive detection of ionic species in aqueous media is of importance for several applications, including environmental monitoring, medical diagnostics, and food analysis.<sup>1,2</sup> One conventional method for monitoring biologically relevant ions (e.g.,  $Na^+$ ,  $K^+$ ,  $Ca^{2+}$ , and  $Cl^-$ ) relies on ionophore-based, ion-selective electrodes (ISEs).<sup>3</sup> The working principle is relatively simple, with the essential part being an ion-selective membrane (ISM) that is able to selectively exchange ions with the analyte solution establishing an interface potential. Essentially, the activity of a (specific) ion dissolved in a solution is converted into an electrical potential, which can be measured by a voltmeter.

In the 1970s, Bergveld pioneered the ion-selective field-effect transistor (ISFET).<sup>4,5</sup> In a FET, an electric field is used to control the shape, and hence the conductivity, of a semi-conducting channel through which charge carriers flow. The conductivity of the channel is not only a function of the applied potential bias between source and drain but also it depends, interestingly, on the surface potential of the channel, the so-called gate, or any layer present onto this channel. Just like in the case of ISEs, the surface potential depends on the ion activity, enabling the use of a FET for detecting ions. Depending on the ion-selective materials present on top of the channel, the FET can be made ion-specific.

FETs have the advantages of being solid-state and microscale, allowing measurements with very short response time.<sup>6</sup> During the past decade, the ISFET concept has been applied to nanoscale devices such as carbon nanotubes,<sup>7</sup> graphene,<sup>8</sup> or nanowires.<sup>9</sup> Due to their reliable and reproducible electrical properties, and the possibility of down-scaling and integration for the simultaneous detection of multiple parameters, silicon nanowire FETs (SiNW-FETs) particularly have gained a lot of interest over the last ~15 years. Examples include ion sensing,<sup>10</sup> label-free biosensing,<sup>11–13</sup> the detection of chemical molecules<sup>14</sup> (e.g., explosives),<sup>15</sup> and disease-related volatile organic compounds.<sup>16–18</sup>

For the detection of distinct ions other than protons, a number of studies have been performed using SiNW-FETs with various types of surface modification. For instance, specific peptides have been utilized for the sensing of  $Ca^{2+}$ ,<sup>19</sup>  $Cu^{2+}$ ,<sup>20</sup> and also for the simultaneous detection of  $Pb^{2+}$  and  $Cu^{2+}$ .<sup>21</sup> In all these cases, the oxide-covered SiNWs were first modified with silanes to form a platform enabling the covalent binding of oligopeptides. Alternatively, a thiol-functionalized silane was used, resulting in devices that showed a high sensitivity to  $Hg^{2+}$ .

Received: October 9, 2014

Accepted: December 9, 2014

Published: December 9, 2014



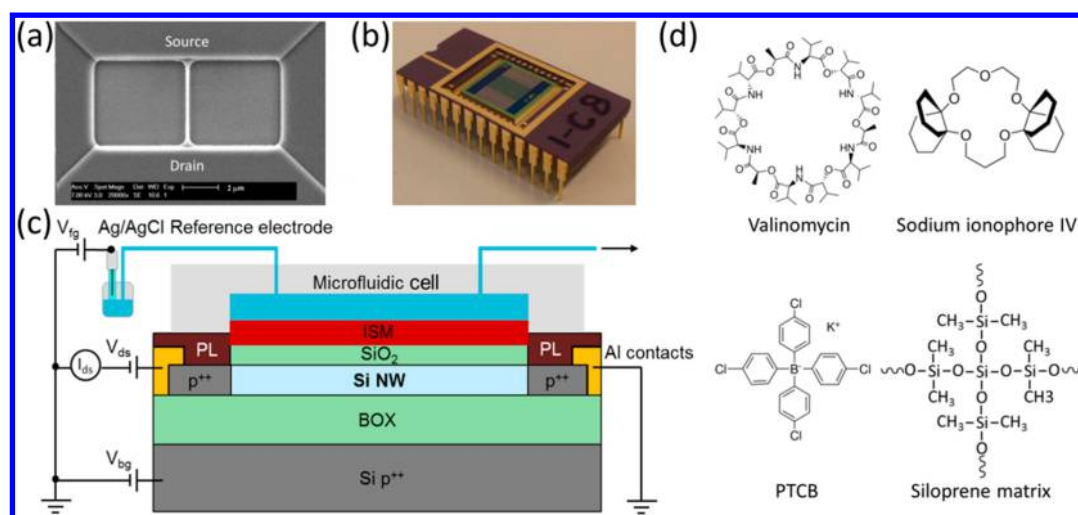


**Figure 1.** (a) Scanning electron microscope (SEM) image of a SiNW (thin vertical lines) with contact areas on the top (source) and bottom (drain). (b) Optical image of a SiNW chip after wire-bonding onto a chip holder. The size of the SiNW chip is  $1 \times 1$  cm. (c) Schematic cross section of the device, including the electrical connections and flow microfluidic device (not to scale). PL is passivation layer. The liquid is delivered by suction to the microfluidic cell by a pump (indicated by the arrow, top right). The Ag/AgCl reference electrode is integrated in the beaker containing the solution to which the nanowire was exposed. The working point of the nanowire transistor is adjusted by two gates: a back-gate voltage  $V_{bg}$  (grounded) and a liquid gate voltage  $V_{lg}$  (applied to the reference electrode). (d) Structures and names of the chemicals used in the preparation of the ISMs.

and  $\text{Cd}^{2+}$  compared to other (hard Lewis acid) cations.<sup>22</sup> Also, crown ethers have been used to prepare SiNW devices for the sensing of  $\text{Na}^+$  and  $\text{K}^+$ . For example, Zhang et al. covalently bound a crown ether derivative onto a Si–C-linked monolayer,<sup>23</sup> while Wipf et al. first covered the SiNWs with gold to immobilize a thiol-functionalized crown ether derivative.<sup>24</sup>

More recently, crown ethers with a high affinity to  $\text{K}^+$  have also been employed to SiNW-based devices via plasticized polyvinyl chloride (PVC) membranes, analogous to the extensive work performed on ISFETs.<sup>5,25</sup> First, Chang et al. reported an extensive study on the extracellular  $\text{K}^+$  monitoring with a valinomycin-coated SiNW device.<sup>26</sup> To this end, a plasticized PVC membrane with a thickness of  $\sim 8 \mu\text{m}$  was prepared via drop-casting onto a chip containing eight devices. The sensitivity of the modified devices covers a broad range of concentrations from  $10^{-6}$  to  $10^{-2}$  M. Second, Schönenberger and co-workers<sup>27</sup> followed the same strategy of surface modification, albeit that they first covered the SiNWs with a layer of  $\text{Al}_2\text{O}_3$  with a thickness of 20 nm. A response of 38 mV/decade was reported. These two PVC-based studies focus on the detection of  $\text{K}^+$  only.

It must be noticed that, compared to covalent surface modification on the SiNW-FETs, a PVC-based membrane made by drop-casting is much easier to handle as less critical pretreatments are required.<sup>28</sup> On the other hand, the lifetime of FETs with a PVC membrane is limited due to the relatively low adherence of the PVC membranes to  $\text{SiO}_2$  surfaces.<sup>29,30</sup> Furthermore, the presence of a plasticizer in the PVC membranes limits the lifetime due to its slow release. Silopren<sup>TM</sup>, a silicon-based polymer, was found to be an interesting alternative to PVC, as it shows a good adhesion to the  $\text{SiO}_2$  surface.<sup>29</sup> Moreover, due to its intrinsic elastomeric properties, siloprene does not require a plasticizer.

In the current study, we report SiNW-FETs modified with two different ionophores incorporated into siloprene for the sensing of alkali metal ions. Taking the advantage of SiNW arrays in a single chip, we separately modified SiNWs with two

different ion-selective membranes (ISMs), in order to simultaneously detect  $\text{K}^+$  and  $\text{Na}^+$ . These ISMs were tested in a conventional ISE configuration as well as on SiNW-FETs, allowing a direct comparison. Results showed a high selectivity and sensitivity for both  $\text{K}^+$  and  $\text{Na}^+$ , thus demonstrating that our device can be used as a multichannel ion sensor.

## EXPERIMENTAL

**Materials and Chemicals.** SiNW-FETs were produced as reported previously.<sup>31,32</sup> Briefly, the SiNWs (p-doped at a concentration of  $10^{16} \text{ cm}^{-3}$ ) are  $3 \mu\text{m}$  in length,  $300 \text{ nm}$  in width, and  $40 \text{ nm}$  in height and were covered with a silicon dioxide gate oxide with a thickness of  $8 \text{ nm}$ . The thickness of the buried oxide (BOX) layer is  $300 \text{ nm}$ . Figure 1a shows a scanning electron microscope (SEM) image of a SiNW. The devices were wire-bonded using conductive glue and gold wires ( $25 \mu\text{m}$  in diameter) with four functional devices per chip (Figure 1b).

Valinomycin (potassium ionophore I), sodium ionophore IV (DD-16-C-5), potassium tetrakis (4-chlorophenyl) borate (PTCB),  $\text{CH}_2\text{Cl}_2$ , siloprene K 1000 (a silanol-terminated polydimethylsiloxane), K-11 (cross-linking agent), KCl, NaCl, agar, and sodium alginate were purchased from Sigma–Aldrich and used as received.

For the sensing experiments we have applied the commonly used mixed-ion solution method, in which at fixed concentration of the interfering ion, the response is measured at different ion concentrations of the primary ion.<sup>33,34</sup> In more detail, the  $\text{Na}^+$  (or  $\text{K}^+$ ) concentration range was prepared by varying the  $\text{Na}^+$  (or  $\text{K}^+$ ) concentration from  $10^{-5} \text{ M}$  to  $10^{-1} \text{ M}$ , while KCl (or NaCl) was added to each solution to obtain a constant ionic strength of  $10^{-1} \text{ M}$ . Sensor responses were plotted as a function of concentration of the primary ion (ion for which the sensor is selective) and not as a function of activity.

**Preparation of Ion-Selective Membranes.** Two types of siloprene membranes were prepared: potassium ion-selective membranes (K-ISMs) and sodium ion-selective membranes

(Na-ISMs). K-ISMs were prepared according to literature.<sup>30</sup> Briefly, approximately a 5:1 weight ratio of valinomycin and PTCB was dissolved in  $\text{CH}_2\text{Cl}_2$ . After this, siloprene K 1000 and K-11 in a 10:1 wt% ratio were added. Also the Na-ISMs were prepared according to literature:<sup>35</sup> a 10:1 weight ratio of sodium ionophore IV and PTCB, dissolved in  $\text{CH}_2\text{Cl}_2$ , were added to a mixture of siloprene K-1000 and K-11. The composition specifications of both types of membranes is given in Table 1.

**Table 1. Composition Specifications of the Two Drop-Casting Solutions Prepared in This Study**

compounds	K-ISM	Na-ISM
valinomycin	3.3 mg (3 $\mu\text{mol}$ )	—
Na ionophore IV	—	3.3 mg (7.3 $\mu\text{mol}$ )
PTCB	0.6 mg (1.2 $\mu\text{mol}$ )	0.3 mg (0.6 $\mu\text{mol}$ )
$\text{CH}_2\text{Cl}_2$	3 mL	1 mL
K-11	35 mg	10 mg
siloprene K 1000	350 mg	100 mg

After stirring the membrane solutions for 10 min, a volume of 0.25 mL was pipetted into a well (11 mm in diameter and 2.5 mm in depth) of a homemade Teflon mold for experiments using the ion-selective electrode (ISE) setup. After the solvent was evaporated overnight, the ISE membranes were gently taken from the mold and placed on a modified ISE tip filled with a 3 M KCl filling solution for the detection of  $\text{K}^+$ , and a 1 M NaCl filling solution in the case of  $\text{Na}^+$  sensing (Figure S-1 of the Supporting Information).

Membranes for the nanowire-based experiments were prepared by drop-casting 5  $\mu\text{L}$  of the membrane solution onto the devices. Then the fluidics were placed on the chips and sealed to prevent leakage of the aqueous solution as described earlier (Figure S-2 of the Supporting Information). To study the thickness of the membranes on the SiNW-FETs, similar droplets were placed on reference  $\text{SiO}_2$  substrates. After drying these membranes, height measurements were performed using a Dektak 8 Stylus Profilometer. The thicknesses of K-ISM and Na-ISM were found to be  $62 \pm 3 \mu\text{m}$  and  $50 \pm 3 \mu\text{m}$ , respectively.

The following approach was used to prepare a drop-casting solution of a hydrogel. First 0.01 g of agar was added to 1 mL of Milli-Q water, followed by the addition of 0.0216 g of sodium

alginate. The mixture was stirred and heated (80  $^\circ\text{C}$ ) for 0.5 h, until a clear solution was obtained. A pipet was used to dropcast 5  $\mu\text{L}$  of the resulting solution onto the SiNW device. After 3 h, an ISM was drop-casted onto the hydrogel-covered device as described above by using 12  $\mu\text{L}$  of the membrane solution. It was observed that the siloprene membrane-containing ionophores (valinomycin or Na ionophore IV) were slightly cloudy after the curing step, most likely resulting from some crystallization of ionophores.<sup>29</sup>

**Electrical Measurements.** The ISE tests were performed using a Metrohm 278 pH lab system with a Metrohm Ag/AgCl reference electrode and a custom-made working electrode (inner electrode is silver/silver chloride), as shown in Figure S-1b of the Supporting Information. The ion-selective electrode has a tip in which the membrane can be (re)placed. For SiNW-FETs measurements, a standard Keithley 4200 semiconductor characterization system equipped with three source measurement units was used for the electrical characterization of the SiNW device during exposure. The device was placed in a specially designed measurement box to ensure more stable source and drain contacts compared to the use of a probe station (Figure S-3 of the Supporting Information). A 50 mV source-drain bias was applied. The drain current ( $I_{\text{ds}}$ ) was measured, while the gate potential was swept. The gate potential can be applied either via the back gate contact ( $V_{\text{bg}}$ ) or an Ag/AgCl electrode in the solution [i.e., the front gate ( $V_{\text{fg}}$ )]. All experiments shown in this paper were performed using a front-gate sweep and keeping  $V_{\text{bg}}$  grounded. From the  $I$ - $V$  plots, we obtained the threshold voltage ( $V_t$ ) at a constant conductance value of 1 nS. It is noted that other parameters can be obtained as well when characterizing SiNW-based devices, including the carrier mobility, the on/off ratio, and the  $I_{\text{sd}}$  at a specific  $V_g$ .<sup>36,37</sup> However, here we have chosen to detect changes in  $V_t$  only as this parameter is directly affected by changes of the boundary potential at the ion-selective membrane solution interface. Figure 1c gives a schematic representation of the measurement setup. The error bars in Figures 2–5 result from 3 subsequent measurements using the same device.

## RESULTS AND DISCUSSION

**ISE Experiments.** Before performing FET measurements, the ISMs were first tested using the conventional ISE setup in order to check the ion-selective properties of the membranes.

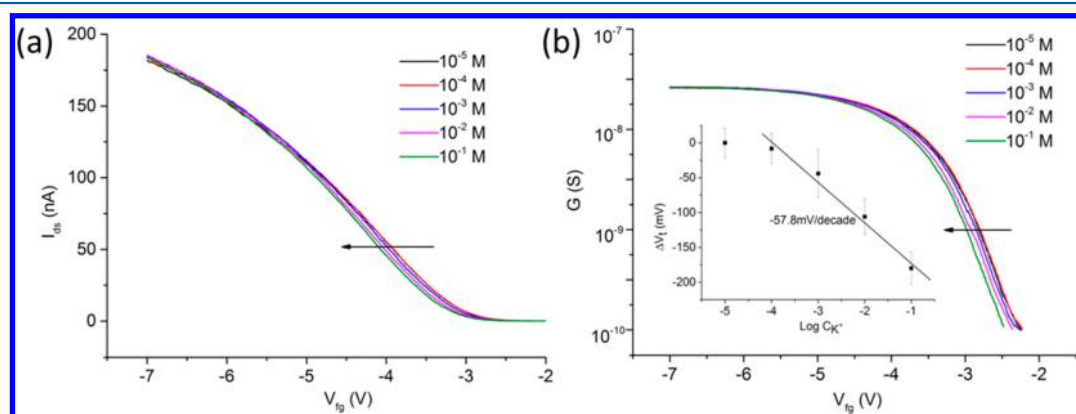


**Figure 2.** (a) Typical  $I_{\text{ds}}-V_{\text{fg}}$  characteristic of one SiNW modified with a K-ISM when exposed to solutions with different  $\text{K}^+$  concentrations and at constant ionic strength. (b) Conductance  $G$  versus  $V_{\text{fg}}$  on a semilog plot for the K-ISM-modified SiNW-based FETs at different concentrations of  $\text{K}^+$ . Inset:  $\Delta V_t$  is a linear function of the logarithmic of the  $\text{K}^+$  concentration with a slope of  $-57.8 \text{ mV/decade}$ .



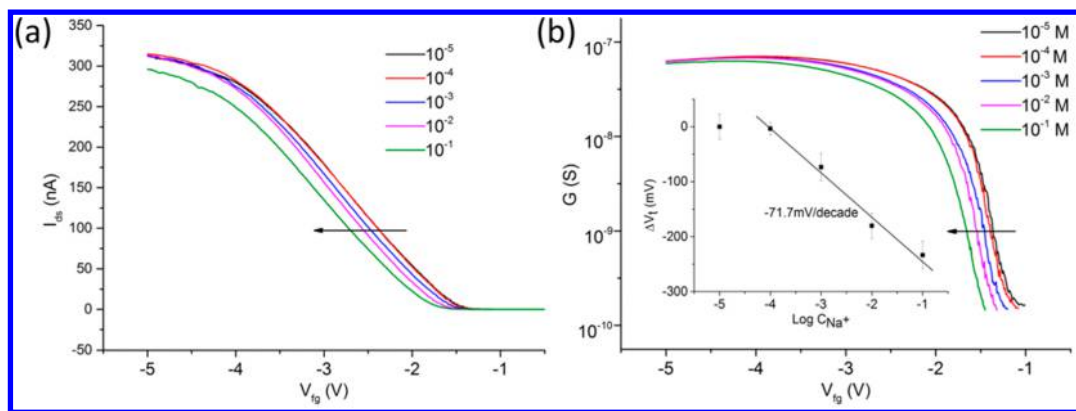


**Figure 3.** (a) Typical  $I_{ds}$ – $V_{fg}$  characteristic of one SiNW modified with a Na-ISM when exposed to a solution with a range of  $\text{Na}^+$  concentrations at constant ionic strength. (b) Conductance  $G$  vs  $V_{fg}$  on a semilog plot for the Na-ISM-modified SiNW-based FETs in different concentrations of  $\text{Na}^+$ . Inset:  $V_t$  is a linear function of the logarithmic of the  $\text{Na}^+$  concentration with a slope of  $-71.7$  mV/decade.

The ionic responses of the potassium ion-selective electrode (K-ISE) were measured toward different concentrations of KCl solutions (from  $10^{-5}$  to  $10^{-1}$  M) at a constant ionic strength ( $10^{-1}$  M). Upon increasing  $\text{K}^+$  concentration, a positive slope was observed of 55 mV/decade in the concentration between  $10^{-4}$  and  $10^{-1}$  M (Figure S-4a of the Supporting Information). This is close to the expected Nernstian slope of  $2.3RT/nF = 59$  mV/decade, where  $R$  is the gas constant,  $T$  the absolute temperature,  $F$  the Faraday constant, and  $n$  the charge of the primary ion.<sup>38</sup> In addition, the Na-ISE gave a linear response toward sodium with a slope of 48 mV/decade over the concentration range from  $10^{-4}$  to  $10^{-1}$  M (Figure S-4b of the Supporting Information), which is comparable to data reported in the literature.<sup>35</sup> All the ISE results indicate that siloprene-based ISMs worked properly.

**SiNW-Based FETs Experiments.** Next we measured the response of ISM-modified SiNW devices to different concentrations of  $\text{K}^+$  and  $\text{Na}^+$ . Figure 2a shows the variation of drain current versus front-gate voltage ( $I_{ds}$ – $V_{fg}$ ) curves of a K-ISM-modified SiNW-FET at different  $\text{K}^+$  concentrations from  $10^{-5}$  to  $10^{-1}$  M and at constant ionic strength. Upon increasing the  $\text{K}^+$  concentration, the curves shift to more negative gate values. This shift is due to the buildup of a positive boundary potential at the ISM interface through the specific adsorption of potassium by valinomycin in the siloprene membrane. In order to keep the  $I_{ds}$  constant, this positive potential has to be compensated by a more negative front gate potential. It is also seen from this plot that the more negative front gate potential is applied, the more electrons are repelled, and the more holes (the majority charge carriers) are present, resulting in an increased  $I_{ds}$ . In order to evaluate the  $V_t$  shifts, the data was replotted in Figure 2b as conductance (i.e.,  $G = I_{ds}/V_{fg}$ ) versus  $V_{fg}$  on a semilog plot. The  $V_t$  was read out the arbitrary values of  $G = 1$  nS as indicated by the arrow in Figure 2b. Next, the normalized  $V_t$  was plotted as a function of the  $\text{K}^+$  concentration (inset Figure 2b). The data clearly show a perfect linear behavior from  $10^{-4}$  to  $10^{-1}$  M, with a slope of  $-57.8$  mV per decade. It should be realized that this slope is related to  $\Delta V_b$  and the  $V_t$  shifts in such a manner to compensate for the change of the ISM boundary potential. Thus a negative slope from the  $V_t$  plot reflects a positive slope of the boundary potential. The slope is very close to the Nernstian response of  $\sim 59$  mV/decade and very much comparable to our result of the performed reference ISE experiment (Section ISE Experiments). The (absolute) slope

we found is closer to the Nernst slope than the one recently reported for a valinomycin-containing PVC membrane onto a gold-coated SiNW device ( $-38$  mV/decade).<sup>27</sup> The only other study on valinomycin-modified SiNW devices reports on changes in conductance rather than  $V_b$ , making it not possible to compare the sensitivities directly.<sup>26</sup>

Next, we studied the hysteresis by comparing the  $V_t$  values obtained from the forward and backward electrical response (Figure S-5 of the Supporting Information). We found a hysteresis effect of  $\sim 30$  mV at a sweep rate of 125 mV/s. A low hysteresis indicates a low density of trapped charges, and recently Haick and co-workers addressed this topic systematically by tuning the density charge of trapping at the  $\text{SiO}_2$  surface.<sup>39</sup> Unfortunately, in most cases the back-gate mode of operation has been used,<sup>11,39,40</sup> making it difficult to compare hysteresis effects quantitatively. Extremely low hysteresis effects have been reported by Vu et al. for pH measurements using a liquid-gated, SiNW-based device, although the sweeping rate details are not mentioned.<sup>41</sup> The hysteresis we found is comparable to the one reported in a recent study on a front-gate operated organic polymer FET.<sup>42</sup>

It should be noted that the timing of the experiments is very important. Although the response of the system at higher concentrations is almost instantaneous ( $<1$  min), the response at the lowest concentrations is much slower (i.e., up to  $\sim 10$  min were needed for the system to stabilize). For that reason, we waited 10 min after changing each concentration, before collecting the  $I$ – $V$  plots to determine the  $V_t$  values. This type of membrane is known to have a detection limit of  $10^{-5}$  M,<sup>43,44</sup> below which the potassium ions leach out of the membrane. The slow response rate can be explained by the equilibration rate from the bulk of the solution through the stagnant layer to the membrane surface (i.e., for lower concentrations in the solution), a lower concentration gradient is present.

The trend in the  $V_t$  shifts observed with the Na-ISM-modified SiNW-FETs is similar to the one of the K-ISM-modified devices. In Figure 3a, the results show that a more negative gate potential has to be applied with increasing sodium ion concentration. We observe that the FET behavior of the devices used to obtain Figures 2 and 3 is different. It is noted that the back-gate mode  $I$ – $V$  characteristics of the devices were already different before the deposition of ISMs. The data presented in Figure 3a was processed to make Figure 3b showing the conductance  $G$  versus the gate potential. The inset shows a linear response with an unexpectedly high slope value

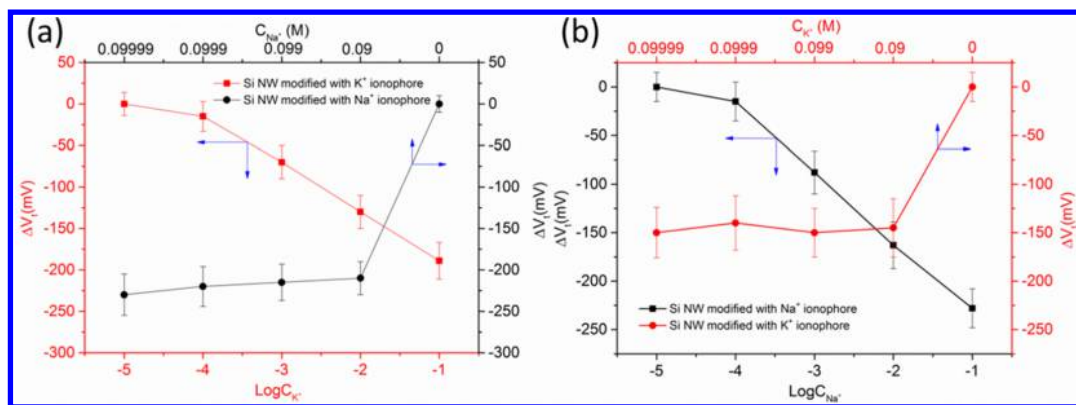


**Figure 4.** Simultaneously testing the concentrations of  $K^+$  and  $Na^+$  in the artificially mixed solutions (with a constant  $[Cl^-]$  and a constant ion strength) by K-ISM- and Na-ISM-modified SiNW FETs. Red curve: threshold shift  $\Delta V_t$  vs  $K^+$  concentration from K-ISM-modified SiNW-based FETs. Black curve: threshold shift  $\Delta V_t$  vs  $Na^+$  concentration from Na-ISM-modified SiNW-based FETs: (a)  $K^+$  concentration varied from  $10^{-5}$  to  $10^{-1}$  M, NaCl was added to adjust the ionic strength to  $10^{-1}$  M and (b)  $Na^+$  concentration varied from  $10^{-5}$  to  $10^{-1}$  M, and KCl was added to bring the ionic strength to  $10^{-1}$  M. Note that the bottom  $x$  axes are logarithmic and that the top  $x$  axes are expanded for ion concentrations  $\geq 0.09$  M.

of  $-71.9$  mV/decade. Before discussing the origin of this high slope, we first present our work on testing the ability of the device to simultaneously detect different types of alkali ions.

To this end, we monitored the  $I$ - $V$  characteristics of a chip containing two sets of nanowires that were covered with two different ISMs in the presence of aqueous solutions containing different concentrations of  $K^+$  and  $Na^+$ . As shown in Figure 4a, upon increasing the  $K^+$  concentration from  $10^{-4}$  to  $10^{-1}$  M, the  $V_t$  of the K-ISM-modified SiNW shifts linearly toward more negative values (red curve). Simultaneously, the response of the Na-ISM-modified SiNW, present on the same chip, did hardly change, which can be understood by the fact that the  $Na^+$  concentration was almost constant [i.e., between 0.09 and 0.09999 M (black curve)]. Finally, in 0.1 M KCl solution, without  $Na^+$  ions being present, the  $V_t$  of the Na-ISM-modified SiNW shifts to a much less negative value. Similarly, a linear  $V_t$  shift of the Na-ISM-modified SiNW was observed for  $Na^+$  concentration between  $10^{-4}$  and  $10^{-1}$  M (Figure 4b, black curve). The response of the K-ISM-modified SiNW is almost constant for  $Na^+$  concentrations between  $10^{-5}$  and  $10^{-2}$  M, while a significant  $V_t$  shift toward a less negative value was observed in 0.1 M NaCl solution due to the absence of  $K^+$  (Figure 4b, red curve). These results demonstrate that  $K^+$  binds to the valinomycin-modified SiNW and  $Na^+$  binds to sodium ionophore-modified SiNW, with a high specificity and without interference, which is in line with ISE studies.<sup>45</sup> This shows that ISM-covered SiNW FETs have a high potential as a multichannel ion sensor.

The findings obtained so far show that the application of ISMs in a conventional ISE and SiNW configuration results in a similar response for  $K^+$ , while the results for  $Na^+$  are quite different. The observed slope value of  $-71.8$  mV/decade for the Na-ISM was unexpectedly high. In an attempt to rationalize it, we first discuss work of Schönenberger's group, reporting that the sensitivity of a dual-gated SiNW-FETs can go beyond the Nernst limit.<sup>46</sup> In their research,  $V_{bg}$  was used to read out  $\Delta G$ , which changed by pH shifts of bulk solution at a fixed  $V_{fg}$ . This resulted in a sensitivity beyond the Nernst limit, due to a larger BOX thickness compared to the front oxide FOX thickness. In our case, however, we varied the front gate potentials, while the back contact was grounded, making our response independent of the BOX thickness.

We note that the Nernst theory describes the thermodynamic behavior of a surface in contact with an electrolyte and that the sensitivity of a SiNW-FET using a liquid gate is fundamentally limited. However, as in our liquid-gate  $Na^+$ /SiNW experiments  $V_t$  shifts more than theoretically expected, and the performances of membranes has been proven by conventional ISE experiments (see ISE Experiments), we conclude that the additional effect must be related to the presence of the SiNW-FETs. It is therefore reasoned that the high slope of  $-71.7$  mV/decade is the result of the summation of two boundary potentials, i.e., the boundary at the Na-ISM solution interface and a boundary potential near the  $SiO_2$  interface. The boundary potential at the Na-ISM interface is expected to be 48 mV/decade as observed for the conventional ISE.

Being aware that the underlying  $SiO_2$  is sensitive to the pH variations, we first checked all the pH values of our testing solutions (Table S-1 of the Supporting Information). After all, in case protons penetrate through the ISM, they may contribute to an additional boundary potential. It turned out, however, that there is no significant difference of pH values in our used solutions. So the effect of protons can be excluded.

The extra (positive) boundary potential may also arise from an equilibration process of sodium ions, which have passed the Na-ISM and entered to some extent the  $SiO_2$ , since it is known that  $Na^+$  can be mobile in  $SiO_2$  insulating layers.<sup>47</sup> To verify this possibility, measurements were done with bare SiNW FETs that were soaked in NaCl solutions with different concentration. In more detail, a device was first soaked in 0.1 M NaCl for 1 h to let the sodium ions equilibrate with the  $SiO_2$  lattice. Then the  $I_{ds}$ - $V_{fg}$  plot was determined. Next, the device was dried and contacted with 0.01 M NaCl + 0.09 M KCl (to keep the ionic strength constant), and the  $I_{ds}$ - $V_{fg}$  plot was measured again. From these plots, a  $+22$  mV/decade shift of  $V_t$  was deduced upon decreasing the NaCl concentration (Table S-2 of the Supporting Information). This corresponds with a decreasing boundary potential of 22 mV/decade. A decrease is indeed expected upon lowering the cation concentration. A value of 22 mV/decade, much lower than expected for Nernstian behavior ( $2.3RT/nF = 59$  mV/dec), might indicate that in the equilibration process between sodium ions at the  $SiO_2$  interface ( $[Na^+]_{interface}$ ) and the sodium concentration

inside the SiO<sub>2</sub> lattice ( $[\text{Na}^+]_{\text{SiO}_2}$ ) is not constant. The Nernst equation for the boundary potential  $E_b$  is given by equation 1:

$$E_b = E^0 + (2.3RT/nF)\log([\text{Na}^+]_{\text{interface}}/[\text{Na}^+]_{\text{SiO}_2}) \quad (1)$$

If the  $[\text{Na}^+]_{\text{SiO}_2}$  slightly increases (i.e., is not constant) with increasing  $[\text{Na}^+]_{\text{interface}}$ , it is seen that by plotting  $E_b$  versus  $\log[\text{Na}^+]_{\text{interface}}$ , the slope will be lower than  $2.3RT/nF = 59 \text{ mV/dec}$ .

Several SiNW-FET studies have reported that various alkali metal cations ( $\text{Na}^+$  and  $\text{K}^+$ ) affect the conductance of bare devices covered with a SiO<sub>2</sub> layer. However, the results are inconsistent. For example, Clément et al. reported a linear Nernstian response to  $\text{Na}^+$  using SiO<sub>2</sub>-covered SiNW-FETs.<sup>48</sup> On the contrary, the response of SiO<sub>2</sub>-coated SiNW-FETs to both  $\text{Na}^+$  and  $\text{K}^+$  reported by Park et al. was found to be nonlinear.<sup>49</sup> It is noted that in these studies, the electrical conductivity was not kept constant, which affects the response.<sup>31</sup> In our case, however, the electrical conductivity of the two solutions is nearly the same.

To obtain additional evidence that this specific interaction between sodium ions and the SiO<sub>2</sub> lattice leads to an additional positive boundary potential, we designed an experiment to keep the  $[\text{Na}^+]_{\text{interface}}$  constant, by the application of a 0.1 M sodium alginate/agar in a hydrogel layer between the SiO<sub>2</sub> interface of the SiNW and the siloprene Na-ISM. The sodium alginate concentration was chosen to prevent the uptake of sodium ions from the solution (no favorable concentration gradient); also, leakage of the sodium ions into the solution is unlikely because of the large size of the alginate polyanion.

The  $I_{\text{ds}}-V_{\text{fg}}$  plots have been recorded for these devices as a function of the sodium ion concentration at constant ionic strength (Figure 5). From these plots, a  $V_t$  shift of  $-58.3 \text{ mV/dec}$

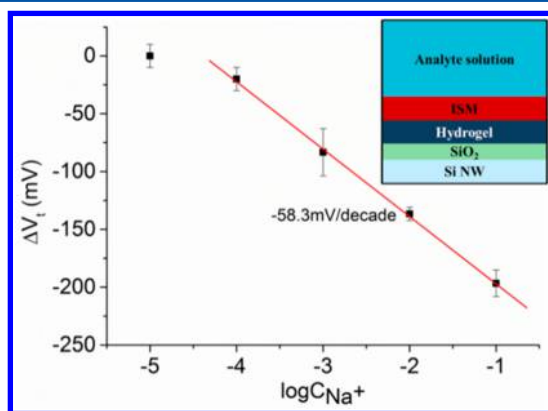


**Figure 5.** Response of the SiNW-based FETs modified with an agar hydrogel (containing 0.1 M sodium alginate) and a Na-ISM. Inset: Schematic cross section of the device after the modification with a sodium alginate-containing agar hydrogel and an ISM (not to scale).

dec is seen upon increasing the sodium concentration. This corresponds with an increasing boundary potential of  $+58.3 \text{ mV/dec}$  at the Na-ISM solution interface. Clearly, it can be concluded that the sodium alginate/agar layer between the SiO<sub>2</sub> and Na-ISM keeps the sodium ion concentration  $[\text{Na}^+]_{\text{interface}}$  constant, resulting in a fixed boundary potential at the SiO<sub>2</sub> interface. Under these conditions, the Na-ISM on the SiNW works perfectly.

Finally, the siloprene-modified SiNW devices have been investigated for their stability in time. During a period of 6 weeks, the ISM-modified, SiNW-based FET devices were

stored in 0.1 M NaCl + 0.1 M KCl. At time intervals of 1 week, the devices were characterized by monitoring the  $I_{\text{ds}}-V_{\text{fg}}$  plot under conditions of 0.01 and 0.1 M of both NaCl and KCl and the shift of  $V_t$  was determined as described previously (Figure S-6 of the Supporting Information). During the whole period, all our modified silicon nanowires kept their ion-sensitive properties, showing that the ISM was present. In addition, the device covered with agar hydrogel and Na-ISM also showed a consistent result within 5 weeks. As a reference experiment, PVC-based ISMs and siloprene-based ISMs were deposited on glass slides. After being soaked in aqueous solutions for 2 h, PVC membranes were slightly detached from the glass surface, while siloprene membranes were still attached. We believe that the stability benefits from the good adhesion between siloprene and the silanol-terminated surface, since a condensation reaction can take place between the silanol and the tetraethoxysilane present in the cross-linking agent.

## CONCLUSIONS

We have demonstrated that SiNW-FETs modified with different siloprene-based ISMs form a promising platform for the sensitive, selective, and simultaneous detection of alkali metal ions. Moreover, the following features endow this method with excellent sensing performances and high stability: (1) the high affinity between the set of two different ionophores and corresponding ions (i.e., valinomycin and Na ionophore IV bind potassium and sodium ions, respectively), (2) good adhesion between siloprene-based membrane and the surface of SiNW-FETs, (3) individually addressable SiNWs on a single chip made by top-down approach. In addition, for the first time, we applied the siloprene-based ISMs on both conventional ISE configuration and SiNW-FETs, which gave us the possibility to directly compare the responses. While the responses to solutions of  $\text{K}^+$  were very much comparable for both sensor systems, the  $\text{Na}^+$  response of the ISM-covered SiNW device was found to be higher than the one of the ISE reference experiment and even higher than Nernstian behavior. We ascribed this to the presence of an additional positive boundary potential due to the interaction between  $\text{Na}^+$  and SiO<sub>2</sub>. We found that the addition of a  $\text{Na}^+$  buffering hydrogel layer between the SiO<sub>2</sub> of the SiNW and the ISM kept the additional positive boundary potential constant. The response was found to be Nernstian as it only depends on the boundary potential of the ISM/electrolyte interface now. Finally, the proposed method shows its potential for multichannel ion sensor applications.

## ASSOCIATED CONTENT

### Supporting Information

Experimental set-up of an ion-selective electrode measurement, and a schematic representation of the tip of a homemade ISE; photographs of a wire-bonded chip and the fluidics; photograph of the setup in which the NW-FETs have been tested;  $\text{K}^+/\text{Na}^+$  response of ionophore/siloprene-modified ISE; hysteresis plot; pH values of different concentrations of NaCl solution with a constant  $\text{Cl}^-$  strength of 0.1 M;  $V_t$  values of bare SiNW-FETs in the presence of different  $\text{Na}^+$  concentrations; long-term stability analysis of SiNW-FETs modified by K-ISMs and Na-ISMs. This material is available free of charge via the Internet at <http://pubs.acs.org>.



## ■ AUTHOR INFORMATION

## Corresponding Author

\*E-mail: l.c.p.m.desmet@tudelft.nl. Tel: +31 152782636. Fax: +31 152788668.

## Notes

The authors declare no competing financial interest.

## ■ ACKNOWLEDGMENTS

The authors would like to thank NanoNextNL, a micro and nanotechnology consortium of the Government of The Netherlands and 130 partners for their financial support. We also thank the reviewers for their helpful and constructive comments. The research was partly carried out under Project M62.3.09339 in the framework of the Research Program of the Materials innovation institute M2i. We thank Sumit Sachdeva, Kai Zhang, and Matija Lovrak (all from TU Delft) for their experimental assistance.

## ■ REFERENCES

- (1) Amine, A.; Mohammadi, H.; Bourais, I.; Palleschi, G. *Biosens. Bioelectron.* **2006**, *21*, 1405–1423.
- (2) Du, J.; Hu, M.; Fan, J.; Peng, X. *Chem. Soc. Rev.* **2012**, *41*, 4511–4535.
- (3) Bakker, E.; Buhlmann, P.; Pretsch, E. *Chem. Rev.* **1997**, *97*, 3083–3132.
- (4) Bergveld, P. *IEEE Trans. Biomed. Eng.* **1970**, *BM17*, 70–71.
- (5) Bergveld, P. *Sens. Actuators, B* **2003**, *88*, 1–20.
- (6) Lee, C. S.; Kim, S. K.; Kim, M. *Sensors* **2009**, *9*, 7111–7131.
- (7) Tans, S. J.; Verschuuren, A. R. M.; Dekker, C. *Nature* **1998**, *393*, 49–52.
- (8) Ang, P. K.; Chen, W.; Wee, A. T. S.; Loh, K. P. *J. Am. Chem. Soc.* **2008**, *130*, 14392–14393.
- (9) Duan, X. F.; Huang, Y.; Cui, Y.; Wang, J. F.; Lieber, C. M. *Nature* **2001**, *409*, 66–69.
- (10) Cui, Y.; Wei, Q. Q.; Park, H. K.; Lieber, C. M. *Science* **2001**, *293*, 1289–1292.
- (11) Stern, E.; Klemic, J. F.; Routenberg, D. A.; Wyrembak, P. N.; Turner-Evans, D. B.; Hamilton, A. D.; LaVan, D. A.; Fahmy, T. M.; Reed, M. A. *Nature* **2007**, *445*, 519–522.
- (12) Huang, Y. W.; Wu, C. S.; Chuang, C. K.; Pang, S. T.; Pan, T. M.; Yang, Y. S.; Ko, F. H. *Anal. Chem.* **2013**, *85*, 7912–7918.
- (13) Zhang, G. J.; Huang, M. J.; Ang, J. A. J.; Yao, Q.; Ning, Y. *Anal. Chem.* **2013**, *85*, 4392–4397.
- (14) Cao, A.; Sudhölter, E. J. R.; de Smet, L. C. P. M. *Sensors* **2014**, *14*, 245–271.
- (15) Engel, Y.; Elnathan, R.; Pevzner, A.; Davidi, G.; Flaxer, E.; Patolsky, F. *Angew. Chem., Int. Ed.* **2010**, *49*, 6830–6835.
- (16) Broza, Y. Y.; Haick, H. *Nanomedicine* **2013**, *8*, 785–806.
- (17) Wang, B.; Cancilla, J. C.; Torrecilla, J. S.; Haick, H. *Nano Lett.* **2014**, *14*, 933–938.
- (18) Konvalina, G.; Haick, H. *Acc. Chem. Res.* **2014**, *47*, 66–76.
- (19) Hitzbleck, M.; Xuan Thang, V.; Ingebrandt, S.; Offenhäuser, A.; Mayer, D. *Phys. Status Solidi A* **2013**, *210*, 1030–1037.
- (20) Bi, X.; Wong, W. L.; Ji, W.; Agarwal, A.; Balasubramanian, N.; Yang, K. L. *Biosens. Bioelectron.* **2008**, *23*, 1442–1448.
- (21) Bi, X.; Agarwal, A.; Yang, K. L. *Biosens. Bioelectron.* **2009**, *24*, 3248–3251.
- (22) Luo, L.; Jie, J.; Zhang, W.; He, Z.; Wang, J.; Yuan, G.; Zhang, W.; Wu, L. C. M.; Lee, S. T. *Appl. Phys. Lett.* **2009**, *94*, 193101.
- (23) Zhang, G. J.; Agarwal, A.; Buddharaju, K. D.; Singh, N.; Gao, Z. *Appl. Phys. Lett.* **2007**, *90*, 233903.
- (24) Wipf, M.; Stoop, R. L.; Tarasov, A.; Bedner, K.; Fu, W.; Wright, I. A.; Martin, C. J.; Constable, E. C.; Calame, M.; Schönenberger, C. *ACS Nano* **2013**, *7*, 5978–5983.
- (25) Jimenez-Jorquera, C.; Orozco, J.; Baldi, A. *Sensors* **2010**, *10*, 61–83.
- (26) Chang, K. S.; Sun, C. J.; Chiang, P. L.; Chou, A. C.; Lin, M. C.; Liang, C.; Hung, H. H.; Yeh, Y. H.; Chen, C. D.; Pan, C. Y.; Chen, Y. T. *Biosens. Bioelectron.* **2012**, *31*, 137–143.
- (27) Wipf, M.; Stoop, R. L.; Tarasov, A.; Bedner, K.; Fu, W.; Calame, M.; Schönenberger, C. In *Transducers*; IEEE: Barcelona, 2013; pp 1182–1185.
- (28) de Smet, L. C. P. M.; Ullien, D.; Mescher, M.; Sudhölter, E. J. R. Organic surface modification of silicon nanowire-based sensor devices. In *Nanowires - Implementations and Applications*; Abbass Hashim (Ed); InTech: Rijeka, Croatia, 2011; pp 267–288.
- (29) van der Wal, P. D.; Skowronskaptasinska, M.; Vandenberg, A.; Bergveld, P.; Sudholter, E. J. R.; Reinhoudt, D. N. *Anal. Chim. Acta* **1990**, *231*, 41–52.
- (30) van der Wal, P. D.; Sudholter, E. J. R.; Boukamp, B. A.; Bouwmeester, H. J. M.; Reinhoudt, D. N. *J. Electroanal. Chem.* **1991**, *317*, 153–168.
- (31) Mescher, M.; Brinkman, A. G. M.; Bosma, D.; Klootwijk, J. H.; Sudhölter, E. J. R.; de Smet, L. C. P. M. *Sensors* **2014**, *14*, 2350–2361.
- (32) Mescher, M.; de Smet, L. C. P. M.; Sudhölter, E. J. R.; Klootwijk, J. H. *J. Nanosci. Nanotechnol.* **2013**, *13*, 5649–5653.
- (33) Morf, W. E. *The Principles of Ion-Selective Electrodes and of Membrane Transport*; Elsevier: New York, 1981.
- (34) Bakker, E.; Meruva, R. K.; Pretsch, E.; Meyerhoff, M. E. *Anal. Chem.* **1994**, *66*, 3021–3030.
- (35) Suzuki, K.; Sato, K.; Hisamoto, H.; Siswanta, D.; Hayashi, K.; Kasahara, N.; Watanabe, K.; Yamamoto, N.; Sasakura, H. *Anal. Chem.* **1996**, *68*, 208–215.
- (36) Bayn, A.; Feng, X.; Muellen, K.; Haick, H. *ACS Appl. Mater. Interfaces* **2013**, *5*, 3431–3440.
- (37) Ermanok, R.; Assad, O.; Zigelboim, K.; Wang, B.; Haick, H. *ACS Appl. Mater. Interfaces* **2013**, *5*, 11172–11183.
- (38) Ruzicka, J. *J. Chem. Educ.* **1997**, *74*, 167–170.
- (39) Paska, Y.; Haick, H. *ACS Appl. Mater. Interfaces* **2012**, *4*, 2604–2617.
- (40) Jang, H.; Lee, J.; Lee, J. H.; Seo, S.; Park, B. G.; Kim, D. M.; Kim, D. H.; Chung, I. Y. *Appl. Phys. Lett.* **2011**, *99*, 252103.
- (41) Vu, X. T.; GhoshMoulick, R.; Eschermann, J. F.; Stockmann, R.; Offenhäuser, A.; Ingebrandt, S. *Sens. Actuators, B* **2010**, *144*, 354–360.
- (42) Knopfmacher, O.; Hammock, M. L.; Appleton, A. L.; Schwartz, G.; Mei, J.; Lei, T.; Pei, J.; Bao, Z. *Nat. Commun.* **2014**, *5*, doi:10.1038/ncomms3954.
- (43) Moss, S. D.; Janata, J.; Johnson, C. C. *Anal. Chem.* **1975**, *47*, 2238–2243.
- (44) Novell, M.; Parrilla, M.; Crespo, G. A.; Xavier Rius, F.; Andrade, F. J. *Anal. Chem.* **2012**, *84*, 4695–4702.
- (45) Qin, Y.; Mi, Y. M.; Bakker, E. *Anal. Chim. Acta* **2000**, *421*, 207–220.
- (46) Knopfmacher, O.; Tarasov, A.; Fu, W.; Wipf, M.; Niesen, B.; Calame, M.; Schönenberger, C. *Nano Lett.* **2010**, *10*, 2268–2274.
- (47) Snow, E. H.; Grove, A. S.; Deal, B. E.; Sah, C. T. *J. Appl. Phys.* **1965**, *36*, 1664.
- (48) Clement, N.; Nishiguchi, K.; Dufrêche, J. F.; Guerin, D.; Fujiwara, A.; Vuillaume, D. *Appl. Phys. Lett.* **2011**, *98*, 014104.
- (49) Park, I.; Li, Z.; Pisano, A. P.; Williams, R. S. *Nanotechnology* **2010**, *21*, 015501.